JOURNAL OF AIRCRAFT
Vol. 36, No. 6, November–December 1999

Technique for Unique Optimization of Dynamic Finite Element Models

Shane A. Dunn*
Defence Science and Technology Organisation, Melbourne, Victoria 3001, Australia

In this paper an optimization procedure, based on a genetic algorithm, is used for the development of a finite element model (FEM) for aircraft structural dynamic analyses. The aim of the optimization was to determine optimal mass and stiffness properties for an FEM of known geometry, such that the FEM results best match known experimental data from ground vibration tests. Fundamental problems with such an optimization for a typical FEM are that many nonunique models can arise or the optimized model does not predict significant experimental features. This issue was addressed here by observing the results of multiple optimizations and determining from the results where such problems arose. It is demonstrated how an investigation of the optimization results can show where such problems arise. Using two case studies, it was then shown how the model complexity in such regions was adjusted to give a unique FEM that predicts all of the significant features found experimentally.

Introduction

A CONTINUING problem in structural dynamics modeling of aircraft structures involves how to best approximate the structure as a finite element model (FEM). Most approaches that have been tried in the past concentrate on modifying the mass and stiffness matrices that result from the FEM, e.g., Refs. 1 and 2, and most of these use modal data, although this has been shown to be insufficient for complete matrix updating in Ref. 3. The work presented here uses frequency response function data and updates the physical properties of the FEM itself, rather than the resulting matrices. The philosophy leading to these decisions is discussed in greater detail in Ref. 4. Much of the work in this field has been concerned with the fact that measured data are typically incomplete because the measurements typically represent fewer freedoms than are represented in the FEM being updated. In previous studies the model complexity typically remains fixed; another way of phrasing this is that the size of the mass and stiffness matrices has remained the same. In the work presented here, the complexity of the FEM is a part of the optimization process.

Recent work[5–7] has demonstrated how the artificial intelligence optimization tool of genetic algorithms (GAs) can be used to create optimal structural FEMs, with optimal being defined as a model that best correlates with the available experimental data. The complexity of the FEM being optimized is of great importance when investigating model optimization procedures. If the model is too complex, the resulting optimized model will be nonunique; if the model is not sufficiently complex, it will not give a satisfactory representation of the real structure. In this paper, a process will be described in which genetic algorithm model optimization processes can be used to achieve unique models of sufficient complexity to give good agreement with the available experimental data. This process will be examined by looking at two case studies: 1) an optimization of a light-aircraft tailplane model based on experimental data and 2) the creation of a beam/mass model of the aft fuselage/empennage of a General Dynamics F111C based on simulated data.

Background

The fundamental approach used to create optimized mathematical models for the structural dynamics of aircraft structures is to determine an optimal set of finite element properties that will give a minimal error between measured frequency response functions and those predicted by the model as described in Eq. (1):

$$\min(\varepsilon(\mu,\kappa)) = \sum_{j=1}^{N}\sum_{i=1}^{n} \| \chi_{i,j}(\mu,\kappa)| - |\chi'_{i,j}\| \tag{1}$$

where the cost function ε, the error between model prediction and measurement, is defined as a function of the mass and stiffness properties μ and κ, respectively. The ε is determined for the model frequency response function $\chi_{i,j}(\mu,\kappa)$ at the ith frequency and jth freedom and the corresponding experimental measurements $\chi'_{i,j}$.

In carrying out this optimization, all of the mass and stiffness properties required for the description of the model are considered to be unknown. (Damping elements are not considered because such elements are rarely included in such FEMs—the inclusion of such elements could well be the subject of further work using these techniques.) The number of properties to be estimated is typically large, and many will have a high degree of interaction; in other words, such a process is typically a high-order, highly nonlinear optimization problem. GAs can be very useful in solving such problems, and for the specific case of structural dynamic model estimation, have been shown to be far more efficient than more traditional optimization processes.[8]

The FEM is prescribed in its geometry, i.e., the nodes are fixed in space, but the physical properties required to describe the mass and stiffness properties are allowed to fall anywhere within a large search space. Stiffness properties may be allowed to range over a number of orders of magnitude, e.g., beam bending stiffnesses may vary from 10^6 to 10^{10} Nm^2. In determining the nature of the FEM to be developed for aircraft structural dynamic analyses, it is typical that an overly complex model is developed; complexity here can be defined as the number of properties required to define the model. In such cases, the following procedure can be carried out:

1) Run the optimization procedure—in this case a GA—a number of times there are a number of results where the better cost functions [Eq. (1)] are very similar and the model predictions give a satisfactory representation of the experimental data.

2) Compare the properties found for these results.

3) Where this comparison shows little variation, assume the property is being determined uniquely.

4) Where the comparison shows a great deal of variation for a similar cost function, assume that either the property is not required, or that the property and one or more of its neighbors can be combined into one.

5) Repeat this process until all parameters appear to be defined uniquely and the model still gives a satisfactory representation of the experimental data.

Received 6 December 1998; revision received 11 May 1999; accepted for publication 13 May 1999.

*Senior Research Scientist, P.O. Box 4331, Airframes and Engines Division, Aeronautical and Maritime Research Laboratory; Shane.Dunn@DSTO.defence.gov.au.

In the first case study tackled in this paper, that of the model optimization for a light aircraft tailplane, it will be demonstrated how this procedure can lead to a very simple model that satisfactorily mimics the experimental data.

There is no point in going beyond the first step in the preceding procedure if, after running the optimization procedure a number of independent times, the initial model configuration does not result in a model that satisfactorily represents the experimental data. If this situation arises, there are three possibilities. 1) The initial model configuration is not sufficiently complex in some regard; 2) the search bounds for the parameters are not sufficient to find a good solution; or 3) the problem is too hard and the optimization has not been allowed to run for a sufficient time to find a satisfactory solution. The second case study investigated here, for the aft fuselage/empennage model of an F111C aircraft, demonstrates such a situation and how it was solved in this instance.

Aerospace Airtrainer CT4 Tailplane

The test article used here was a tailplane for a CT4, a propeller-driven military trainer and the same set of data is used here as was used in Ref. 6. The tailplane was mounted on springs and 2-kg masses added at the tips. Band-limited white noise (0–100 Hz) loading was applied at the tip and accelerations were measured with a roving accelerometer at the six locations on the semispan shown in Fig. 1. The transfer functions between these accelerometer readings and the measured load input were determined and are shown in Fig. 1. Three modes can be seen in these transfer functions, two below 10 Hz and one at about 40 Hz. The lowest frequency mode is rigid body roll of the tailplane on the springs, the next is rigid body heave, and the highest mode is the first bending mode. The transfer functions at the frequencies marked in Fig. 1 were used as the points to be best matched in the model optimization process.

Optimization of 12 Physical Parameters

The first attempt at optimizing the FEM using a GA for this problem involved optimizing the properties for the model as shown in Fig. 2. These properties were the six masses shown: five beam stiffnesses and the spring stiffness—a search in 12-dimensional space. The search space for each of the parameters was set over a very wide range on the basis that as few as possible a priori assumptions should be used. Very quick analyses showed that the search space could be reduced to the following bounds: the bending stiffness EI for each of the beams was allowed to vary between 50×10^3 Nm^2–350×10^3 Nm^2 (E is the elastic modulus and I is the cross-sectional area moment of inertia of the representative beam); the masses at each point were allowed to vary between 0–7 kg; and the mounting spring stiffnesses varied between 14×10^3 N/m–19×10^3 N/m. The bounds for beam stiffnesses and mass were still left deliberately quite wide, whereas those for the spring stiffnesses were readily identified as lying within a relatively small search space.

After running the GA a number of times, it was found that the results for the cost function tended to fall into two regions: One where the cost function fell in the range 1.2–2, and another where the cost function was around 6.5. As finding the results with a low cost function is the aim, the results with ε [Eq. (1)] > 2 were discarded. The remaining results for the bending stiffness and mass distribution found for independent runs of the GA are shown in Fig. 2. As can be seen, the bending stiffnesses and masses are not well characterized because even though the cost function does not vary greatly, the optimized masses and stiffnesses cover a wide range. There is some useful information contained in these results because the mass at the tip seems to be relatively well identified and there is a tendency for there to be a significant mass at node 4; beyond this, however, there is little hard information to be gleaned from these results. The real meaning in results such as these is that the model depicted in Fig. 2 is too complex for the available measurements to be used to optimize this many parameters uniquely. Another indicator toward this conclusion is the way in which adjacent points in the curves in Fig. 2 tend to vary in a high-low-high or low-high-low manner. This means that the optimization routine may simply require the sum of these properties to be an average of the two values.

When carrying out such optimizations, it is always worthwhile to look at the fitted results to ensure that the routine is behaving properly. As has been stated, two distinct sets of results were found in the optimization carried out here. The fitted function results from each of these sets are shown in Figs. 3 and 4. The results shown in Fig. 3 show that the nonunique optimized model gives a very good fit so that the optimization procedure is working well. The results shown in Fig. 4 are interesting because they show the result found for an attractive local minimum in the cost function. It can be seen that the local minimum arises because the bending mode of the tailplane is relatively well modeled, but the results at lower frequencies clearly do not match so well.

As has been shown, the attempt to optimize the model involving 12 physical parameters using the available measurements results in

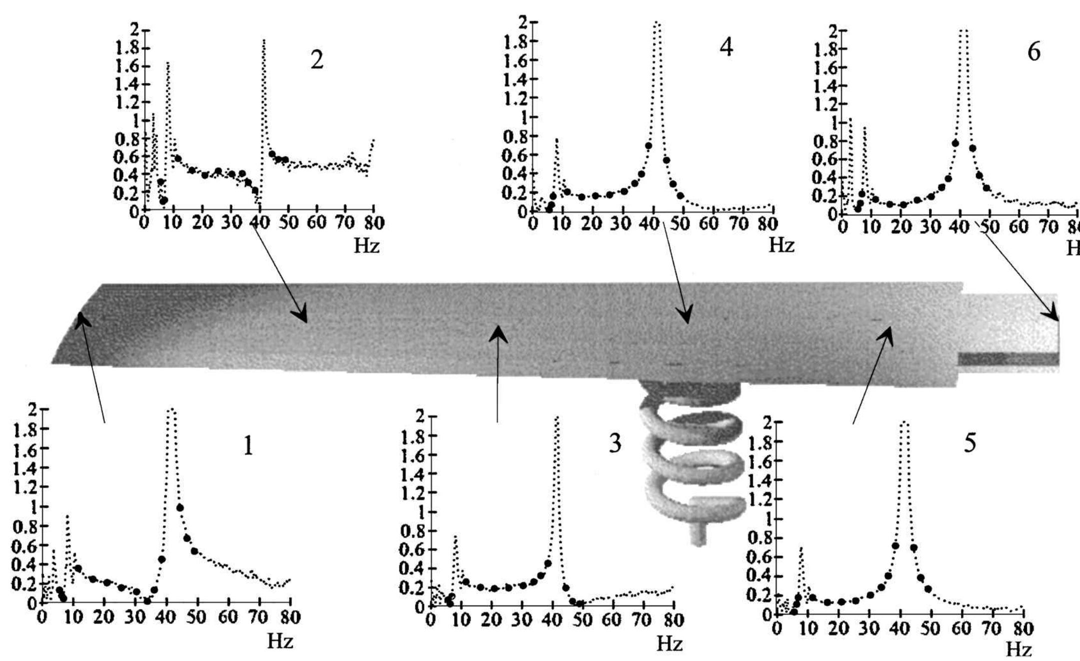

Fig. 1 Transfer functions for the six degrees-of-freedom measured along the semispan. The solid circles indicate the points used in the subsequent optimization procedure.

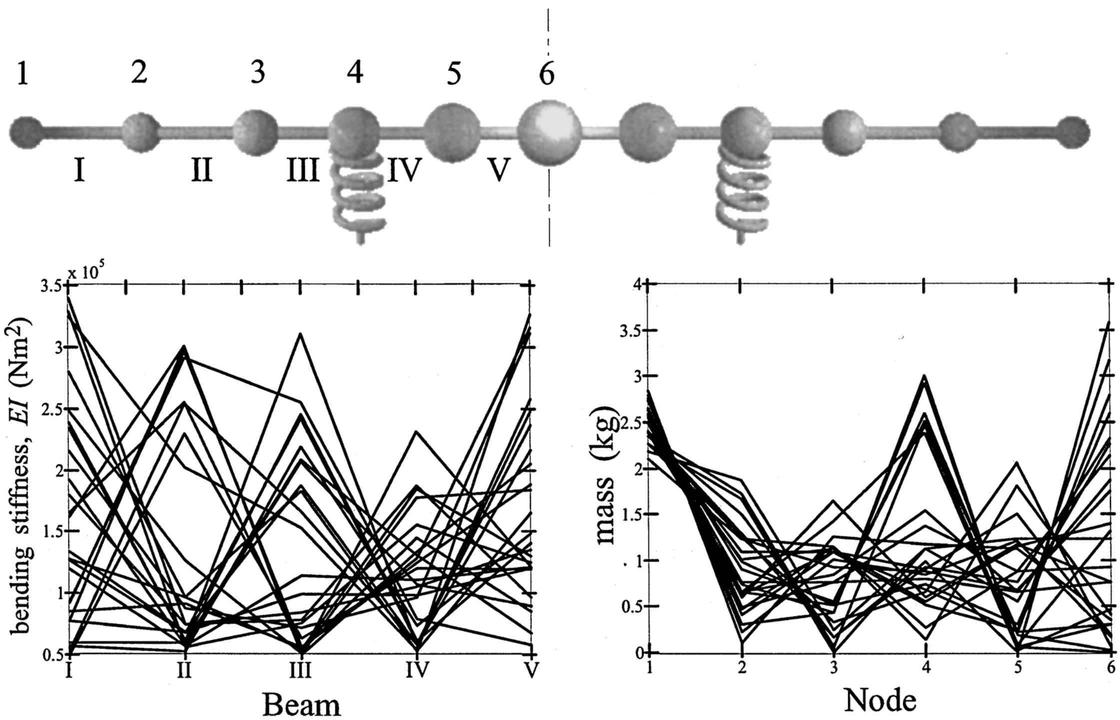

Fig. 2 Finite element representation of the model being optimized for the case of five beams, six masses, and one spring stiffness and the results for the beam stiffness and mass distribution found by several runs of a GA.

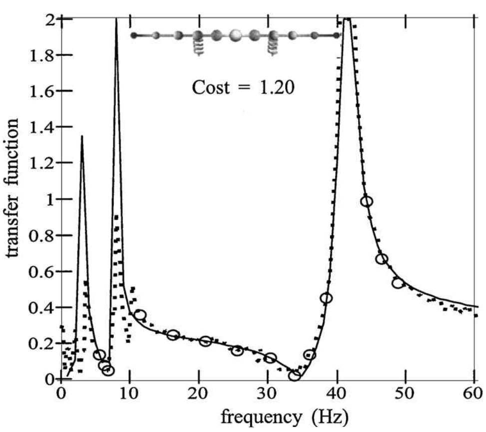

Fig. 3 Model prediction and measurements at the tip for the best model found for the optimization of the model as shown in Fig. 2.

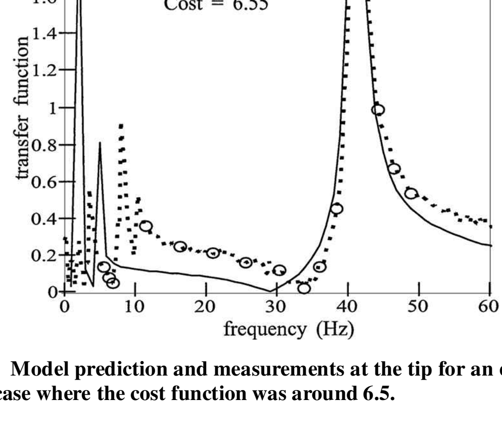

Fig. 4 Model prediction and measurements at the tip for an example of the case where the cost function was around 6.5.

a nonunique representation. One way around this uniqueness problem is to use more measurements that have already been collected. As can be seen in Fig. 3, however, the optimized model seems to fit the measurements reasonably well, even at the frequencies not used in the optimization procedure. Therefore, it seems unlikely that adding any of these measurements will add a great deal of information. Another possibility is to collect more measurements, either at more locations or at higher frequencies. Given that the first bending mode is a simple shape, it is likely that the six measurement locations are sufficient to characterize the deformation that is occurring. It is unlikely that higher spatial resolution will offer significantly more information. Exciting the structure to higher frequencies will give rise to features such as panel vibration that cannot be modeled using such a stick/mass model and is therefore likely to create spurious effects in the optimization. It is also worth keeping in mind that one of the main aims of the exercise is to create optimal models for aeroelastic analyses for which such high frequency behavior is typically of little importance. Another means of arriving at a unique model is to reduce the complexity of the model.

Optimization of Seven Physical Parameters

The model complexity was reduced to that shown in Fig. 5 with three beams, three masses, and one spring stiffness to be optimized. The limits for each of the properties were as those used in the previous section.

The results for the beam stiffness and mass distribution found by several runs of a GA shown in Fig. 5 tend to show that a unique identification has not been made. The beam stiffness results exhibit a large degree of the high–low behavior seen in the results in the previous section whereas the tip mass appears reasonably well identified with the masses at nodes 4 and 6, appearing to be exhibiting some nonuniqueness. These results, however, contain no information as to the cost function associated with each of the solutions. At this point, it can be useful to look at scatter plots of the various properties found plotted against the value of the cost function. These plots are shown in Fig. 6.

The results for the beam stiffnesses in Fig. 6 show that beams I and III are tending toward a unique solution with improving cost function whereas the results for beam II are scattered widely. Each

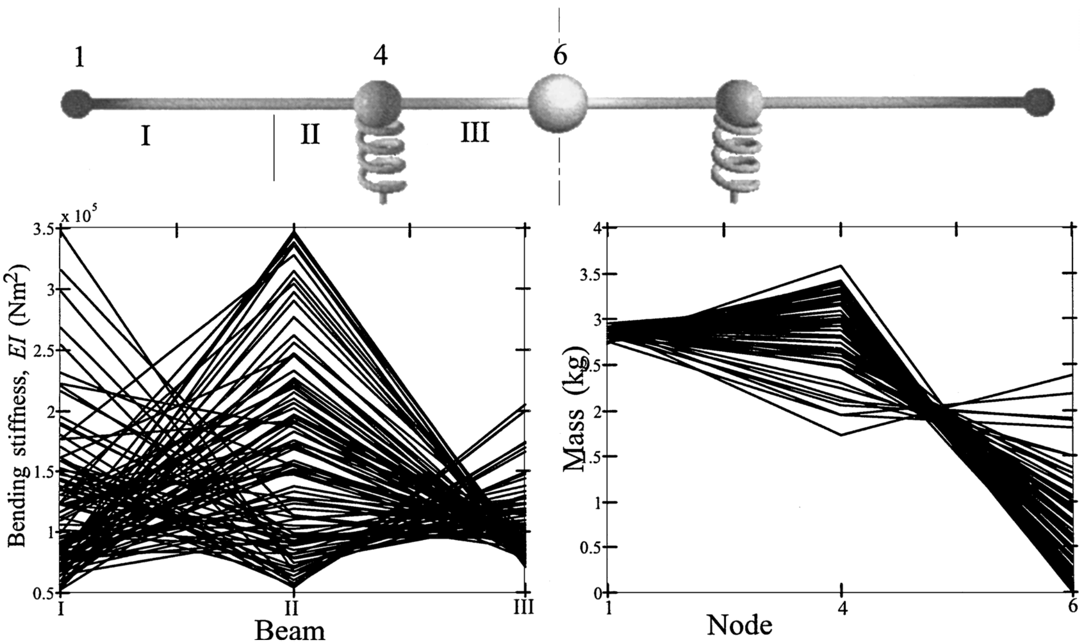

Fig. 5 Finite element representation of the model being optimized for the case of three beams, three masses, and one spring stiffness and the results for the beam stiffness and mass distribution found by several runs of a GA.

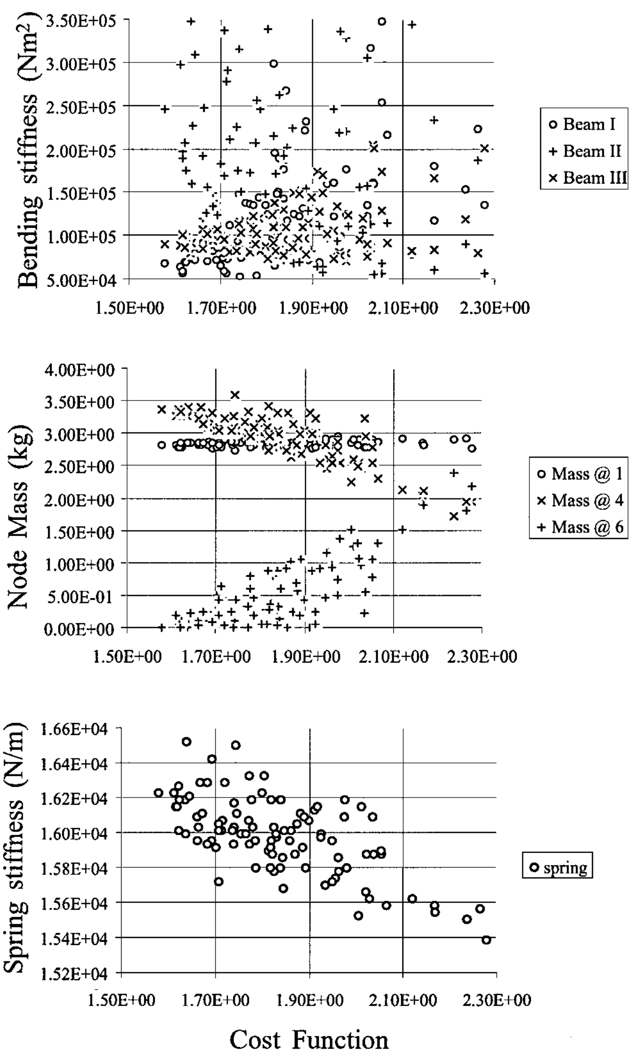

Fig. 6 Scatter plots of estimated properties against cost function for the case of three beams, three masses, and one spring stiffness.

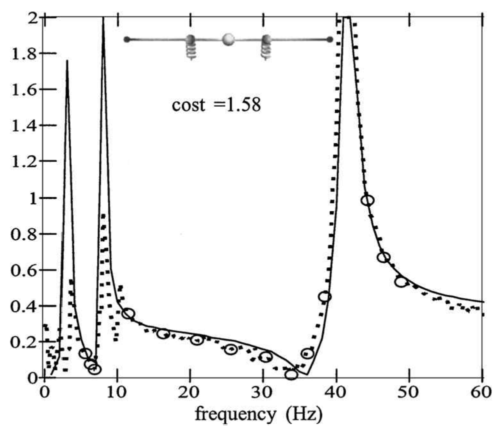

Fig. 7 Model prediction and measurements at the tip for the best model found for the optimization of the model as shown.

of the masses show good convergence, notably with the mass at node 6 tending toward zero. The results for the spring stiffness also show very good convergence.

Again, it is important to compare the estimated model behavior against the measured properties to ensure that nothing unexpected is occurring within the frequency range of interest. This comparison for the tip freedom is presented in Fig. 7. As can be seen in Fig. 7, the optimized model still gives an adequate representation of the structural behavior, but as shown in Fig. 5, is still nonunique.

Optimization of Five Physical Parameters

The model was further reduced to two beams, two masses, and one spring stiffness. A problem that can arise here involves the placement of the masses and the location of the change in beam properties. Results from the previous section seem to suggest that a mass at the tip is important (not surprising considering that the configuration being tested had a substantial mass added at the tip). It is not clear, however, that a mass at node 4 is optimal; it is quite possible that a mass at nodes 3 or 5 could give better results. Even worse, there is no clue as to where, with two beams, the optimal location for a change in beam properties should be. To overcome these difficulties, three additional unknowns were added to the problem: the placement of the first mass (first being defined as that closest to the tip); the placement of the second mass; and the location of the change in beam properties. Each of these properties is constrained to be at one of the predefined node locations as defined by the measurement locations. The five physical properties and the three locations to be found amount to a search in eight-dimensional space. The form of the model to be optimized is shown in Fig. 8. The scatter plots for the optimized parameters plotted against cost function are shown in Fig. 9.

The scatter plots for the beam stiffnesses in Fig. 9 are interesting in that the optimal stiffnesses for the two beams almost converge to the same number, although there is a tendency for beam I to have a greater stiffness than beam II. These results can be related to the last plot, which shows the nodal position for the change in stiffness. The scatter shown in this plot is not surprising for beams of almost equal stiffness, though the best results undergo a change in stiffness at node 5—the location of the cutout in the tailplane shown in Fig. 1. The scatter plots for the two masses clearly converge well and the plots for the nodal locations of these masses show only one pair of solutions being found. As for all the previous runs, the mounting spring stiffness is well identified. The optimized model

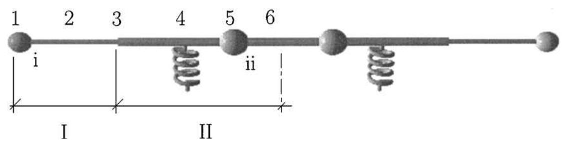

Fig. 8 Finite element representation of the model being optimized for the case with two beams, two masses, and one spring. The masses were free to be placed at any of the six nodes and the beam properties were free to change at one of nodes 2–5.

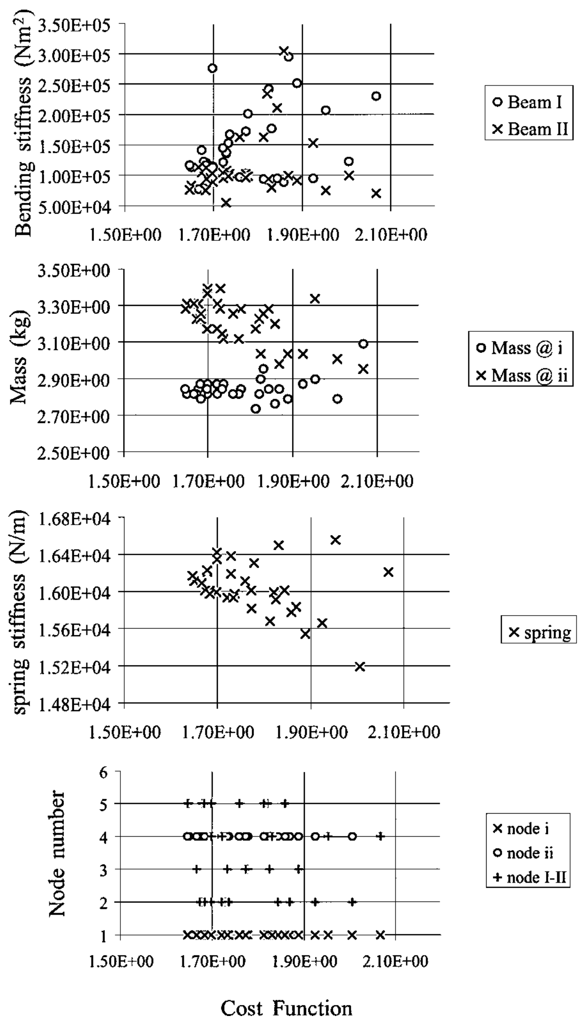

Fig. 9 Scatter plots of estimated properties against cost function for the case of two beams, two masses, and one spring stiffness.

and the model prediction compared with the experimental data are shown in Fig. 10.

General Dynamics F111C Aft Fuselage/Empennage Symmetric Model

General Dynamics created a very detailed FEM of the F111C based on modeling the detailed structure including spars, ribs, and skins. For dynamic analyses, the mass and stiffness matrices created by this FEM were analytically reduced to 80 degrees-of-freedom for the model with symmetric boundary conditions. These 80×80 matrices were acquired by the Australian Department of Defence for aeroelastic analyses of Australia's F111C fleet. For the purposes of the analyses carried out here, these reduced matrices have been used to create simulated ground vibration test (GVT) frequency response functions. The mass distribution for the original model is shown in Fig. 11.

The aim here was to take the simulated frequency response functions and attempt to develop a beam/mass FEM that will give a good approximation to these data. The model from General Dynamics is fully constrained at a point on the fuselage just aft of the wing attachment. This has the effect of breaking the model into two: a forward fuselage/wing model and an aft fuselage/empennage model. The development of the beam/mass model for the full aircraft is covered in Ref. 7; presented here is the aft fuselage/empennage model-making process to demonstrate a situation where the initial model

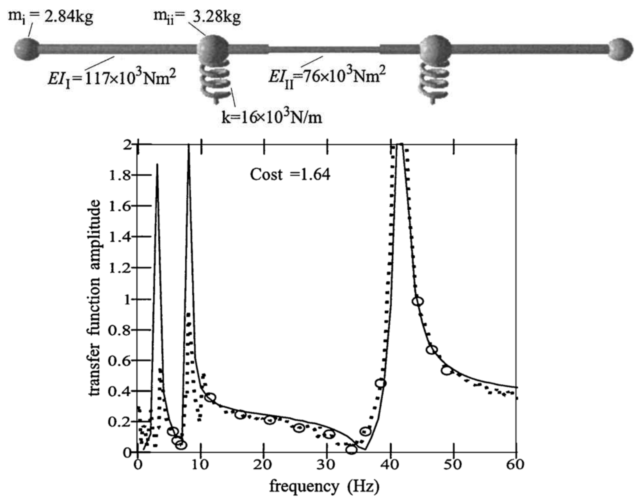

Fig. 10 Model prediction and measurements at the tip for the best model found for the optimization of the model as shown.

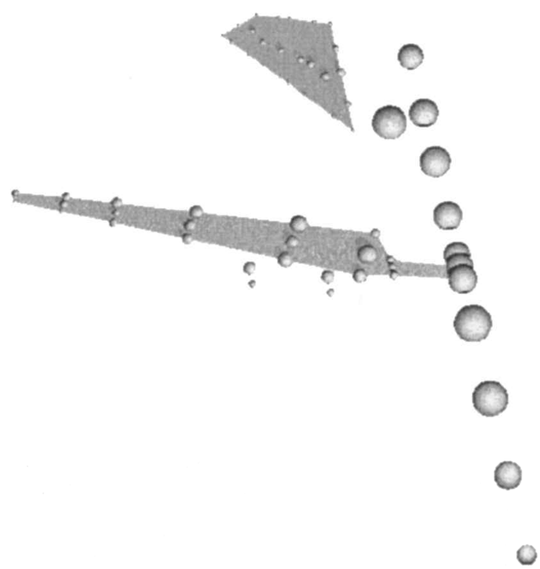

Fig. 11 Mass distribution for General Dynamics F111C reduced model (the shaded areas simply denote the plane of the wing and tailplane).

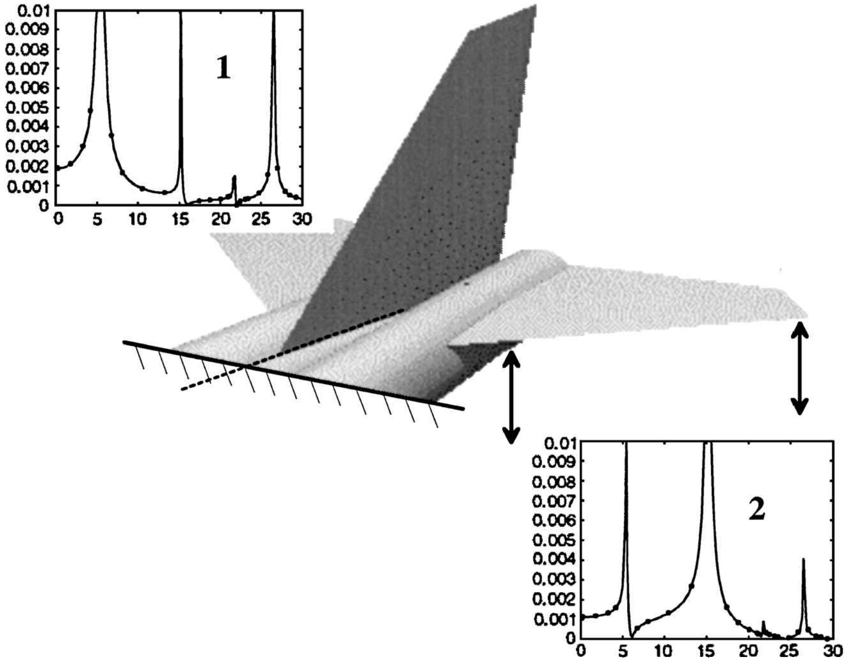

Fig. 12 Diagram showing aft fuselage/empennage of an F111C as represented in that part of the General Dynamics model. Simulated GVT measurements were taken at 16 degrees-of-freedom, two of which are shown here: 1, aft fuse tip heave; and 2, stabilator tip heave.

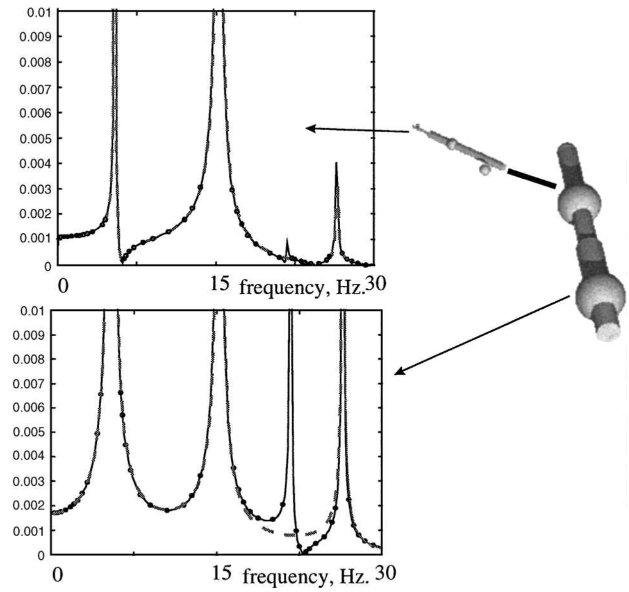

Fig. 13 Initial aft model configuration showing stabilator tip heave (top graph) and fuselage heave (the dashed line shows the optimized model results).

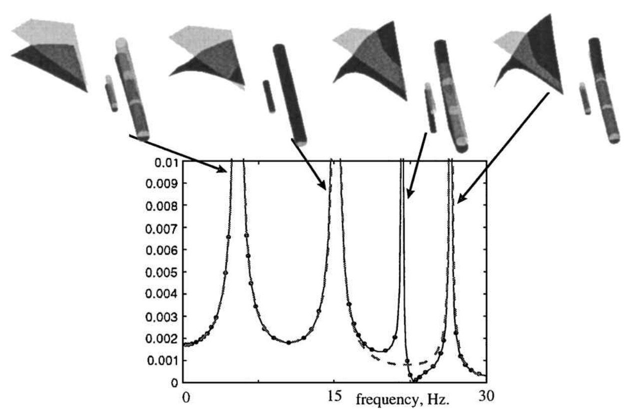

Fig. 14 Diagram showing the four modes of vibration of the aft fuselage/empennage model based on the original General Dynamics model.

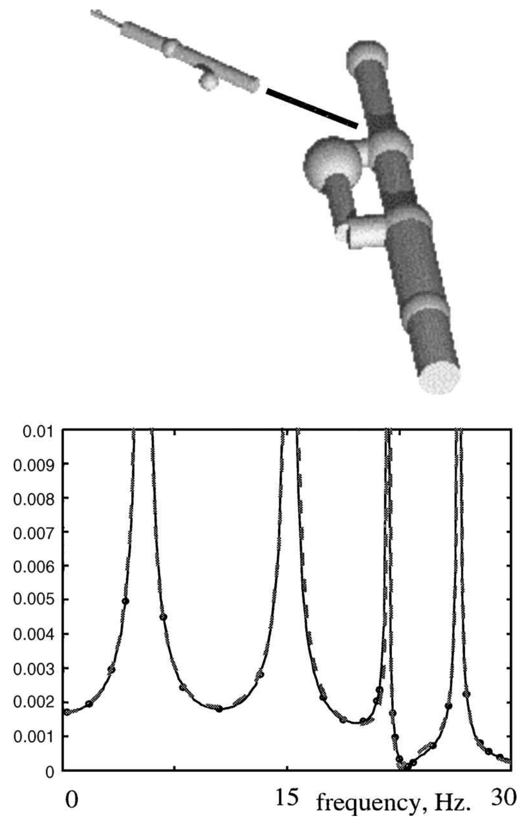

Fig. 15 Aft model configuration showing the optimized model predictions (- - -) and the original model data for a heave freedom on the fuselage.

configuration was not sufficiently complex to model the measured behavior.

The simulated data are gathered by applying sinusoidal loads at the locations shown in Fig. 12 and collecting the frequency response functions at a range of freedoms, two of which are shown in this figure (Sixteen measurement freedoms were used in the analysis of the aft fuselage/empennage model.)

The model optimization procedure used for the aft fuselage/empennage model of the F111 is the same as was described for the tailplane model optimization. The layout of the model is as depicted in Fig. 13 with the fuselage and stabilator modeled as beams and lumped masses. The initial representation required the optimization of 46 unknown parameters. As can be seen for the model predictions shown in Fig. 13, the stabilator tip behavior seems to be well modeled, but examination of a freedom on the fuselage makes it clear that a mode is not being represented.

Having a feature of the experimental data not being represented by the model resulting from the optimization procedure in this manner suggests that the initial model representation was not sufficiently complex. To investigate the manner in which the model configuration should be changed to better predict the measured behavior, the nature of the four modes of vibration in this frequency range was examined, as shown in Fig. 14.

As can be seen in Fig. 14, the main feature of the mode not being modeled is that it contains significantly more engine motion than the other modes. For the first model configuration, it was intended that the engine could simply be represented as an added mass on the fuselage center line; the results shown in Fig. 14 clearly suggest this was wrong. The configuration was therefore changed to model the engine explicitly, as shown in Fig. 15, and the whole procedure repeated. The resulting optimized model predictions for the heave freedom on a fuselage node are also shown in Fig. 15. The final model required the optimization of 31 properties.

Conclusions

The question of model uniqueness is one of the most significant issues arising from FEM improvement studies that have been carried out in the past. This usually arises because, typically, very complex FEMs are being modified. There is usually insufficient information when using experimental data to modify such complex mathematical models. If, however, a process of model creation is used in which the experimental data in the region of interest are an inherent part of that model-making process, then it is possible to develop a model of just sufficient complexity to represent the behavior of interest. Such a process has been demonstrated here based on multiple runs of a GA optimization. The model complexity is varied as the process continues, and the form of the FEM that gives a good representation of the observed experimental behavior with the minimum number of properties is taken as the unique model.

The process of changing the complexity of the model was carried out manually. Work now needs to be carried out in which model complexity becomes an implicit part of the optimization procedure such that minimal intervention is required by the analyst.

References

[1] Baruch, M., "Optimal Correction of Mass and Stiffness Matrices Using Measured Modes," *AIAA Journal*, Vol. 20, No. 11, 1982, pp. 1623–1626.

[2] Kabe, A., "Stiffness Matrix Adjustment Using Mode Data," *AIAA Journal*, Vol. 23, No. 9, 1985, pp.1431–1436.

[3] Baruch, M., "Modal Data are Insufficient for Identification of Both Mass and Stiffness Matrices," *AIAA Journal*, Vol. 35, No. 11, 1997, pp. 1797, 1798.

[4] Dunn, S. A., "The Use of Genetic Algorithms and Stochastic Hill-Climbing in Dynamic Finite Element Model Identification," *Computers & Structures*, Vol. 66, No. 4, 1998, pp. 489–497.

[5] Dunn, S. A., "The Use of Genetic Algorithms in Dynamic Finite Element Model Identification for Aerospace Structures," *Proceeding of the 20th Congress of the International Council of the Aeronautical Sciences*, AIAA, Reston, VA, 1996, pp. 398–406.

[6] Dunn, S. A., "Modified Genetic Algorithm for the Identification of Aircraft Structures," *Journal of Aircraft*, Vol. 34, No. 2, 1997, pp. 251–253.

[7] Dunn, S. A., "Optimization of the Structural Dynamic Finite Element Model of a Complete Aircraft," *Proceedings of the 21st Congress of the International Council of the Aeronautical Sciences*, ICAS-98-4-9-3, Sept. 1998.

[8] Dunn, S. A., "Optimal Genetic Algorithm Properties for Dynamic Finite Element Model optimization," *Computers & Structures*, Vol. 66, No. 4, 1998, pp. 489–497.